A NEW LAMBERTSON MAGNET FOR THE FNAL 400 MeV LINAC

J.-F. Ostiguy*, H.D. Glass, D.J. Harding, J. Lackey, W. Robotham
Fermi National Accelerator Laboratory, Batavia, IL 60510, USA †

Abstract

A new Lambertson magnet has been constructed for use at the downstream end of the Fermilab 400 MeV Linac. To reduce costs, the core is composed of laminations left over from the Main Injector dipoles with a round hole through one pole face. In contrast with more conventional Lambertson designs, the magnet is excited by two coils located above and below the field region. The integrated transverse fringe field at the end of the field-free region is minimized using a pole piece extension with 75% packing factor followed by a thick flux return plate. The relatively low packing factor prevents saturation of the extension by the return flux while preserving the odd longitudinal symmetry of the transverse flux distribution. Measurements show better than an order of magnitude reduction of the integrated transverse field, in good agreement with simulations.

INTRODUCTION

In this paper, we present the design rationale and the result of simulations and measurements performed on a new magnetic septum magnet of the Lambertson type. This magnet will be located at the downstream end of the Fermilab 400 MeV linac. By default, the linac H^- beam circulates through the field-free region of the magnet, into a spectrometer magnet and finally, to a beam dump. For injection into the Booster synchrotron, the beam is first kicked vertically into the bending region of the Lambertson and then horizontally into an injection stripping chicane.

Historical Background

In 1993, the Fermilab Linac was upgraded from 200 to 400 MeV by replacing the last four tanks of the original drift-tube Linac (which provided acceleration from 116 to 200 MeV) with 805 MHz side-coupled cavities (four times the original frequency). Raising the Booster injection energy reduced emittance growth by providing a reduction in space-charge tune-shift and improvements in magnetic field quality by reducing the relative importance of remanent magnetization and eddy currents. Coincidentally with commissioning of the upgraded linac, production of new dipole magnets for the Main Injector had just begun. Because of a tight schedule and a desire to minimize costs, a DC Lambertson magnet was build using readily available Main Injector dipole laminations. Since the beam circulating through the field-free region is directed to a dump, minimum attention was paid to end field effects beyond the addition of crude shielded extensions. Not surprisingly, it was later found that despite the presence of these extensions, the dipole kicks experienced by the beam in the end regions remained substantial enough to steer the beam away from the dump. Dipole correctors were installed; however, both operationally and from a safety point of view, they are somewhat of a nuisance because the excitations need to be carefully readjusted following every shutdown. A decision was made to build an improved version of the magnet, with the constraint that the lamination geometry should not be modified.

DESIGN CONSIDERATIONS

Lambertson magnets are typically used for extraction in high energy machines. For this application, the normally circulating beam traverses a field-free region, basically an opening carved into one of the poles of a dipole magnet. At extraction, an upstream pulsed kicker magnet moves the beam vertically (horizontally) into the dipolar field region (i.e. the so-called bending region) where it is deflected horizontally (vertically) into an extraction beamline. In practice, kicker magnets have limited strength, and the magnetic septum needs to be as thin as possible. The minimum thickness is obviously limited by saturation which causes penetration of the flux into the field-free region. To retard the onset of saturation, the field free region opening often has a characteristic V-shaped notch to take maximum advantage of the smaller diameter of the (higher energy) extracted beam.

The Lambertson magnet described in the paper is used for injection. The field-free opening has a simple 44.5 mm (1.75 in) diameter circular shape to accommodates a 5 mm-mr (95%) beam. At 400 MeV, kicker strength is less of an issue and the magnetic septum has a minimum thickness of 5.56 mm (0.219 in). Furthermore, since the beam makes only a single pass through the field-free region, field quality requirements are not as stringent as they would be for a storage ring.

An important consideration for Lambertson magnets is the effect of fringe field in the end regions. Magnetic flux lines originating from the opposite pole have a tendency to terminate on the interior of the field-free opening since it is at the same magnetic potential as the pole it is carved into. If no special measures are taken, a strong transverse magnetic field is present at the extremities of the field-free region. Since this field has an asymmetric and nonlinear dependence on radial offset, its presence can lead to serious perturbations. To mitigate fringe field effects, two approaches are possible. The obvious one is a complete suppression of the fringe field. This can be accomplished

* ostiguy@fnal.gov
† Work supported by the US Department of Energy under contract number DE-AC02-76CH03000.

Figure 1: *View of an extremity with the end plate removed.*

Figure 2: *Shield plate at the lead-end extremity.*

by making the surface of the pole containing the field-free region completely flat, extending it a few gap lengths beyond the end of the other pole and by providing a high permeability path for the flux to return before it reaches the edge of field-free aperture [3]. The second possibility is to force the magnetic field in the end regions to be predominantly longitudinal [1, 2]. This can be done by placing a thick shield (a steel plate which mirrors the field-free opening) at a small distance away from the end of the magnet. The flux leaves one of the poles and enters the shield at

Figure 3: *Shield plate at the non lead-end extremity.*

normal incidence; it then circulates around the openings and back into the opposite pole. If the plate permeability is high, its surface is a magnetic equipotential and the field vanishes downstream from it. In the gap between the end of the field-free region and the corresponding opening in the shielding plate, the magnetic field has a transverse component. However, the latter possesses an odd longitudinal symmetry with respect to the center of the gap. In practice, this symmetry becomes more exact as the distance between the pole end and the shielding plate is reduced, the relevant dimension being the thickness of the septum. Making the gap very small is generally not an option because it increases the flux circulating through the shield and saturates it, rendering it ineffective. To preserve both the odd longitudinal symmetry of the transverse magnetic field and to avoid saturation of the shield plate, the space between the end of the field-free region and the plate can be filled with (magnetically) loosely packed laminations.

Because it was not possible to modify the existing magnet core, the second approach was selected. Magnetic shielding plates were build out of solid 7.6 cm (3 in) thick steel. To allow for in-tunnel assembly and disassembly, each plate is made out of two pieces approximately of the same size, horizontally joined together. At both magnet extremities, the field-free pole is extended by 9.8 cm (3.850 in) using alternating laminations of 1.5 mm (0.0598 in) steel and 0.5 mm (0.020 in) G-10, yielding a 75% packing fraction. The shielding plate mechanically rests on the end of the extension.

SIMULATIONS AND MEASUREMENTS

To model the magnet and optimize the shield thickness and the packing factor of the field-free pole extension, we used OPERA3D [4], a standard FEM magnetostatics code. Only one end was modeled, assuming a somewhat simplified end plate geometry very similar to that of the entrance plate (lead-end). Note that the exit plate geometry is somewhat different due to the large bend angle (9.9 deg) and the need to accommodate vacuum connections and other neighboring hardware. The shielding plate geometries are shown in Figures 2 and 3. To gain some confidence and as a reference to assess the effectiveness of the end effect mitigation scheme, we first measured and modeled a bare rectangular end as shown in Fig. 1. The results are presented in Fig 4. Following a few iterations (both computational and experimental) a satisfactory geometry was attained. It is likely that further optimization could lead to even better performance, but this was not pursued. Figure 5 shows contours of the magnetic field magnitude in a shielding plate which does not have sufficient thickness. The area where saturation occurs (in red) indicates the importance of providing enough width. When the plate is not magnetically equipotential, a characteristic long transverse field tail is produced. Figure 6 shows measured (using a Hall probe) and computed transverse magnetic field at the end of the field-free region for the final geometry (the origin coincides

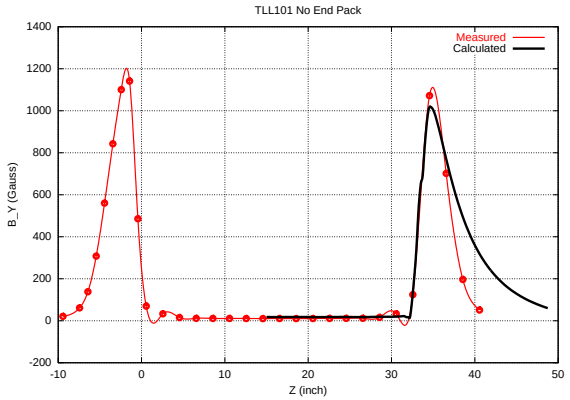

Figure 4: *Measured transverse magnetic field in absence of endpacks. The integrated magnetic field is 240 G-m. The calculated field is also shown for comparison.*

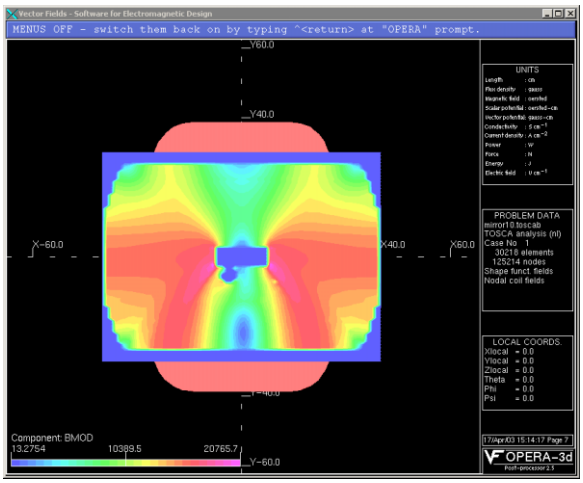

Figure 5: *Calculated flux magnitude distribution in the shielding plate, assuming a field-free extension of 4.125 in, 75% packing factor and a plate thickness of 0.75 in.*

with the surface of the shielding plate). At the center of the field-free region, the field is almost exclusively longitudinal. At ± 0.375 in vertical offset, a pattern resulting from the curving of the field lines near the edges of the circular aperture is observed. The odd symmetry is nearly perfect in the direction away from the septum and a little bit worse in the opposite direction. Compared with a simple rectangular end, the measured integrated transverse field strength is reduced by a factor of 12 i.e. from 240 to 19 G-m.

DISCUSSION AND CONCLUSION

Reduction of fringe-field effects at the extremities of the field-free region of a Lambertson magnet is a common problem. The strategy presented in this paper allows one to reduce the magnitude of the transverse field perturbation by one and possibly up to two orders of magnitude. However, a longitudinal component of roughly the same amplitude as the uncorrected transverse one remains. In applications

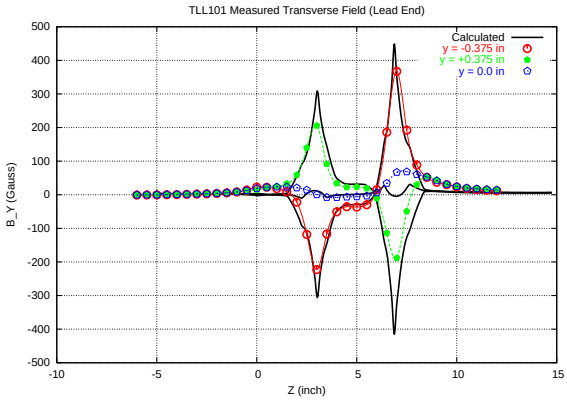

Figure 6: *Transverse magnetic field in the field-free region measured at different radial offsets.*

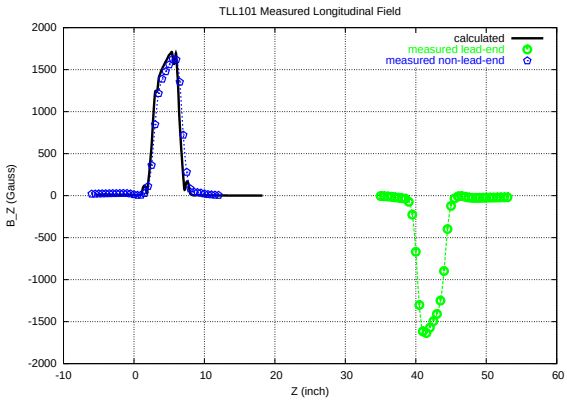

Figure 7: *Measured longitudinal magnetic field in the field-free region. The calculated field is also shown for comparison.*

where the beam normally circulates through the field-free region, the presence of this longitudinal component may introduce small amounts of transverse coupling and focusing whose impact on beam dynamics needs to be quantified and taken into consideration.

REFERENCES

[1] J.-F. Ostiguy and D.E Johnson, “3D End Effects in Iron Septum Magnets”, Proceedings of the 1995 Particle Accelerator Conference, Dallas, TX, pp. 1349-1351

[2] D.E. Johnson et al., “Design and Magnetic Measurements of the Fermilab Main Injector Lambertson”, Proceedings of the 1997 Particle Accelerator Conference, Vancouver, Canada, pp. 3272-3274

[3] N. Tsoupas et al., “Design and B-Field Measurements of a Lambertson Injection Magnet for the RHIC Machine”, Proceedings of the 1995 Particle Accelerator Conference, Dallas, TX, pp 1352-1354

[4] OPERA, Vector Fields Ltd, Oxford, UK